NANO LETTERS

2008
Vol. 8, No. 3
794-799

Direct Deposition of Trivalent Rhodium Hydroxide Nanoparticles onto a Semiconducting Layered Calcium Niobate for Photocatalytic Hydrogen Evolution

Hideo Hata,[†,§] Yoji Kobayashi,[†] Vince Bojan,[‡] W. Justin Youngblood,[†] and Thomas E. Mallouk*[,†]

Department of Chemistry and Materials Research Institute, The Pennsylvania State University, University, Park, Pennsylvania, 16802

Received October 5, 2007; Revised Manuscript Received January 20, 2008

ABSTRACT

Well-dispersed $Rh(OH)_3$ nanoparticles were deposited in the interlayer galleries of a Dion−Jacobson type layered perovskite ($ACa_2Nb_3O_{10}$: A = H or K). X-ray photoelectron spectra and ζ potential measurements suggest covalent bonding (Rh−O−Nb) between the nanoparticles and the niobate sheets. After calcination of $Rh(OH)_3/KCa_2Nb_3O_{10}$ at 350 °C in air, interlayer $Rh(OH)_3$ nanoparticles were transformed to Rh_2O_3 and showed higher photocatalytic activity for hydrogen evolution using methanol as a sacrificial electron donor.

The direct photochemical cleavage of water to generate hydrogen and oxygen has been studied since the early 1970s[1] and still attracts considerable interest today because of its potential for low-cost solar energy conversion.[2] A number of metal and metal oxide catalysts (e.g., NiO_x,[3] RuO_2,[4] $Rh_{2-y}Cr_yO_3$,[5] Rh-Cr_2O_3,[6] Pt[7]) deposited on wide band gap semiconducting materials have been investigated in this context. Layered oxides (e.g., $Na_2Ti_3O_7$, $K_2Ti_4O_9$, $K_2La_2Ti_3O_{10}$, $K_4Nb_6O_{17}$, and $KCa_2Nb_3O_{10}$)[8] are interesting wide band gap semiconductors for photocatalytic reactions because they readily intercalate water and because ion-exchange reactions can be used to deposit noble metal cocatalysts at specific interlayer sites. In most of these materials, however, intercalation reactions are limited to cationic guest species. Ebina et al. reported that Pt or cationic Ru clusters could be loaded onto sheets of the layer perovskite $KCa_2Nb_3O_{10}$ by precipitation with strong base and the restacked high surface area composites showed high activity for water splitting.[9] However, it is still very challenging to control the dispersion of such catalytic nanoparticles on the host semiconductor sheets. Although we recently succeeded in intercalating noble metal nanoparticles into layered oxides by first intercalating coordinating polyamines,[10] in that case, there was no direct bonding between the nanoparticles and the host layers, which is important for redox catalysis.

In this paper, we report the direct deposition of $Rh(OH)_3$ nanoparticles, which can be converted to catalytic Rh_2O_3 nanoparticles by calcination, into the interlayer of $HCa_2Nb_3O_{10}$ or $KCa_2Nb_3O_{10}$. Surprisingly, the reaction appears to involve covalent bonding of the clusters to the sheets, and this results in uniform dispersion of nanoparticles even at high loading.

Intercalation of Nanoparticles. The Rh_2O_3-loaded photocatalyst was prepared by exfoliation and intercalation of proton-exchanged $KCa_2Nb_3O_{10}$ (see Supporting Information for details). $HCa_2Nb_3O_{10}$ (0.13 g) was exfoliated by shaking in 50 mL of aqueous tetra(*n*-butyl)ammonium hydroxide (TBAOH) (25.0 mM) for 1 month. To obtain 1.5 wt % loading of $Rh(OH)_3$, which corresponds to 1 wt % loading of Rh, 20 mM aqueous $RhCl_3$ (0.632 mL) was added to 50 mL of the exfoliated TBAOH/$Ca_2Nb_3O_{10}$ suspension (pH ∼ 12.0) together with methanol (10 vol %), followed by photoirradiation with a 300 W Xe lamp for 18 h. The loading was adjusted by changing the amount of $RhCl_3$ solution. Immediately after adding the red $RhCl_3$ solution to the TBAOH/$Ca_2Nb_3O_{10}$ suspension, the color of the sheets in the suspension became lemon yellow, which is typical of $Rh(OH)_3$ under basic conditions.[11] After the intercalation reaction, the yellow suspension was dispersed in 2 M KOH solution to precipitate the restacked $Rh(OH)_3/Ca_2Nb_3O_{10}$

* Corresponding author. E-mail: tom@chem.psu.edu.
† Department of Chemistry, The Pennsylvania State University.
‡ Materials Research Institute, The Pennsylvania State University.
§ Present address: Shiseido Research Center (Shin-Yokohama), Shiseido Co. Ltd., 2-2-1 Hayabuchi, Tsuzuki-ku, Yokohama, 224-8558, Japan.

10.1021/nl072571w CCC: $40.75
Published on Web 02/12/2008

sheets while exchanging the interlayer cations from TBA^+ and H^+ to K^+. If excess $RhCl_3$ solution was used (beyond a Rh loading of 24.7 wt %), the supernatant solution remained yellow, and peaks attributed to $Rh(OH)_3$ were observed in the XRD pattern in addition to peaks from $Rh(OH)_3/Ca_2Nb_3O_{10}$ (see Supporting Information, Figure S1). The solid obtained is designated $Rh(OH)_3/KCa_2Nb_3O_{10}(n)$, where n denotes the Rh loading in wt %. To transform the interlayer $Rh(OH)_3$ nanoparticles to Rh_2O_3, $Rh(OH)_3/KCa_2Nb_3O_{10}$ was heated at 623 K for 1 h in air. The calcined samples are abbreviated $Rh_2O_3/KCa_2Nb_3O_{10}(n)$. The formation of Rh_2O_3 was apparent as a color change from yellow to dark brown after calcination. $Rh_2O_3/KCa_2Nb_3O_{10}$ as well as $Rh(OH)_3/KCa_2Nb_3O_{10}$ were tested as photocatalysts for hydrogen evolution in aqueous methanol solutions.

XRD patterns show that $Rh(OH)_3$ nanoparticles can be intercalated without photoirradiation (see Supporting Information, Figure S2), and the materials so obtained had almost the same photocatalytic activity as those made by photoirradiation. However, the maximum loading was less than 10 wt % Rh without photoirradiation; in contrast, the supernatant remained colorless at higher loadings, implying more Rh intercalation, with photoirradiation.

Figure 1 compares XRD patterns of $HCa_2Nb_3O_{10}$, $TBAOH/Ca_2Nb_3O_{10}$, and $Rh(OH)_3/KCa_2Nb_3O_{10}$ composites at different loadings (0.1, 1.0, and 10.0 wt %). In the intercalated samples, only 00*l* and *hk*0 reflections were present, indicating turbostratic restacking of the sheets. The interlayer spacings of $HCa_2Nb_3O_{10}$ and $TBAOH/HCa_2Nb_3O_{10}$ prior to the deposition were 1.45 and 2.57 nm, respectively, and the estimated *d*-spacings of $Rh(OH)_3/KCa_2Nb_3O_{10}$ (0.1, 1.0, and 10.0 wt %) were 1.60, 1.66, and 1.99 nm, respectively. This layer expansion relative to $HCa_2Nb_3O_{10}$ implies intercalation of $Rh(OH)_3$ nanoparticles in the interlayer gallery. Subtracting the thickness of the calcium niobate layer (1.16 nm),[12] the gallery heights were 0.44, 0.50, and 0.83 nm for $Rh(OH)_3/KCa_2Nb_3O_{10}$ (0.1, 1.0, and 10 wt %), implying that the intercalated nanoparticles are less than 1 nm in diameter. We did not observe any diffraction peaks that could be attributed to $Rh(OH)_3$, which is evidence that crystalline aggregates of $Rh(OH)_3$ do not form in the galleries. In addition, the decrease in gallery height relative to $TBAOH/Ca_2Nb_3O_{10}$ indicates that TBA^+ and residual H^+ cations were substituted by K^+ ions after washing with KOH solution. The loss of TBA^+ was confirmed by FT-IR spectra in which the C−H stretching vibration (2800−3000 cm^{-1}), clearly visible in the TBA^+ intercalated material, was not observed in $Rh(OH)_3/KCa_2Nb_3O_{10}$ (see Supporting Information, Figure S3). Analytical data for samples restacked with KOH showed no significant difference (K/Ca/Nb mole ratio 0.8/2.3/3.0 in both cases) between 0 and 10 wt % Rh loaded samples. This indicates that $Rh(OH)_3$ that is bound to the niobate sheets is ionizable in base and that the overall ion exchange capacity is the same after loading with $Rh(OH)_3$.

Typical TEM images of $Rh(OH)_3/KCa_2Nb_3O_{10}$ (1.0 and 10.0 wt %) are shown in Figure 2. Even at high loading, the $Rh(OH)_3$ nanoparticles were well dispersed within the galleries. From the TEM images, the estimated average

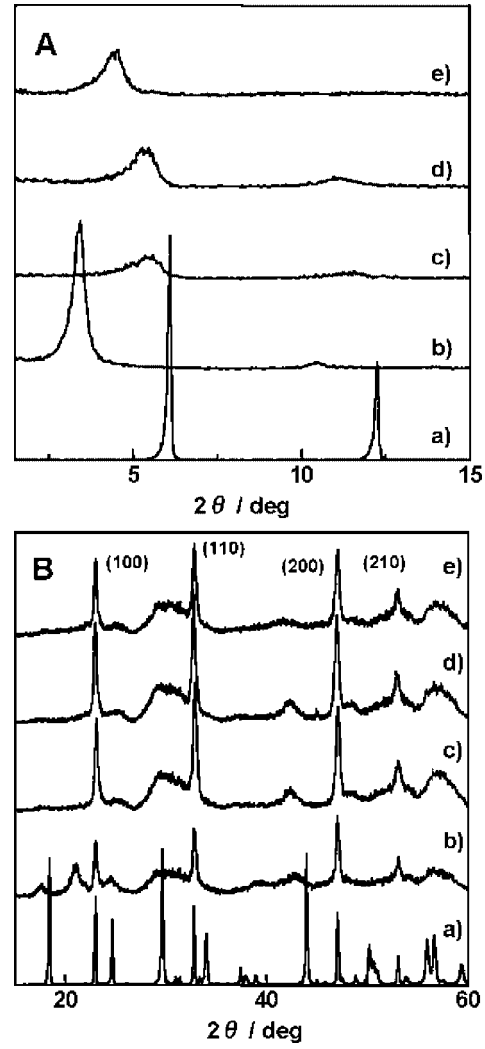

Figure 1. XRD patterns in the low 2θ region (A) and higher angle region (B) of $HCa_2Nb_3O_{10}$ (a), $TBAOH/HCa_2Nb_3O_{10}$ (b), and $Rh(OH)_3/KCa_2Nb_3O_{10}$ with different Rh loadings (0.1 wt %) (c), (1.0 wt %) (d), and (10.0 wt %) (e).

particle diameters in $Rh(OH)_3/KCa_2Nb_3O_{10}$ (at 1.0 and 10.0 wt %) were 0.7 ± 0.2 and 1.1 ± 0.3 nm, respectively. The increase of the average particle size with the loading is consistent with the expansion of *d*-spacing observed in XRD measurements (Figure 1). EDX spectra showed Rh in all areas sampled in TEM imaging, consistent with the apparent uniform dispersion of $Rh(OH)_3$ nanoparticles.

We previously reported that $HCa_2Nb_3O_{10}$ can be topochemically dehydrated by heating to 463–573 K.[13] To avoid this irreversible transformation, interlayer TBA^+ and H^+ ions were replaced by K^+ by reaction with aqueous KOH. The presence of K^+ was confirmed by EDX in the TEM imaging. Figure 3 shows XRD patterns of $Rh_2O_3/KCa_2Nb_3O_{10}$ (0.1, 1.0, 10.0 wt %) obtained by calcining $Rh(OH)_3/KCa_2Nb_3O_{10}$. After calcination, the basal spacing of $Rh_2O_3/KCa_2Nb_3O_{10}$ (0.1, 1.0, 10.0 wt %) decreased to 1.54, 1.54, and 1.66 nm, respectively (Figure 1), which is still somewhat larger than that of $KCa_2Nb_3O_{10}$ (1.42 nm). The extra gallery height can again be attributed to intercalated nanoparticles, in this case Rh_2O_3. Again, no diffraction features that could be attributed to Rh_2O_3 were evident in the XRD patterns,

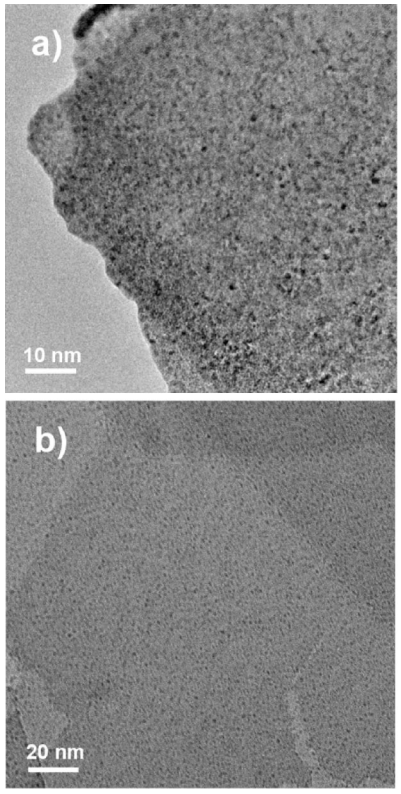

Figure 2. TEM images of $Rh(OH)_3/KCa_2Nb_3O_{10}$ (1.0 wt %) (a) and (10.0 wt %) (b).

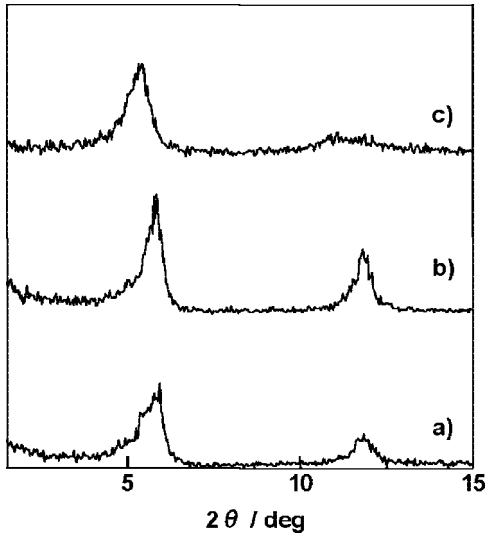

Figure 3. XRD patterns of $Rh_2O_3/KCa_2Nb_3O_{10}$ (0.1 wt %) (a), (1.0 wt %) (b), and (10.0 wt %) (c).

meaning that regardless of the loading of $Rh(OH)_3$, aggregation of the intercalated nanoparticles does not occur during calcination.

Covalent Interactions Between Rh-Oxide Nanoparticles and Niobate Sheets. Because oxide-supported noble metal and metal oxide nanoparticles tend to coalesce and crystallize upon calcination, the persistent dispersion of subnanometer Rh_2O_3 particles in the niobate galleries is unusual. Another unusual observation was the insensitivity of these nanoparticles to cation exchange in 2 M KOH. It had previously been reported that cationic CrO_x nanoparticles could be intercalated into the layered titanate $Ti_{1.83}O_4$, which was first exfoliated by reaction with TBAOH.[14] On this basis, we expected $Rh(OH)_3$ nanoparticles to intercalate under conditions of pH where their net charge was positive. When $Rh(OH)_3$ was intercalated at saturation coverage (initial Rh loading of 24.7 wt %), IR spectra showed that most of the TBA^+ ions were displaced from the galleries without subsequent treatment with 2 M KOH (see Supporting Information, Figure S3). Therefore, our initial impression was that the interaction between $Rh(OH)_3$ and the $Ca_2Nb_3O_{10}$ sheets was primarily electrostatic.

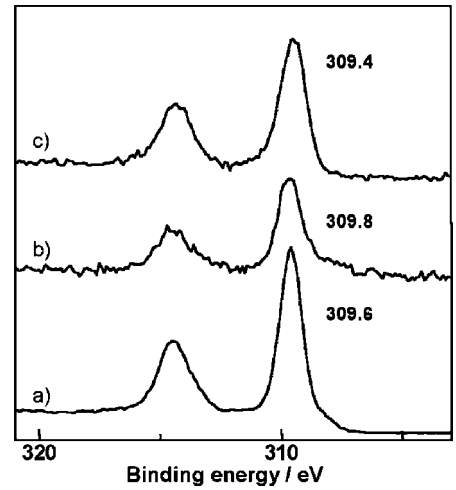

Figure 4. XPS spectra in the Rh 3d region of $Rh(OH)_3$ (a), $Rh(OH)_3/KCa_2Nb_3O_{10}$ (10 wt %) (b), $Rh_2O_3/KCa_2Nb_3O_{10}$(10 wt %) (c). Spectra are referenced to adventitious carbon at 285.0 eV.

Zeta potential measurements of $Rh(OH)_3$ nanoparticles[15] at pH 5.0 to 13.0 (see Supporting Information, Figure S4) showed that their isoelectric point was about pH 7.0. Thus, the nanoparticles have a negative surface charge at pH 12.0, which is the pH of the intercalation reaction. Because the $Ca_2Nb_3O_{10}$ sheets are also negatively charged at high pH, the $Rh(OH)_3$ nanoparticles cannot be anchored in the galleries by electrostatic forces. Even at high loading, $Rh(OH)_3$nanoparticles are not displaced by reaction with aqueous KOH, but under these conditions, TBA^+ cations are completely removed. As a control experiment, we attempted to intercalate $Rh(OH)_3$ nanoparticles into an exfoliated fluoromica,[16] which also has negative layer charge at high pH but which has no Nb atoms or surface OH groups. In this case, XRD patterns showed no evidence of $Rh(OH)_3$ intercalation. Although some $Rh(OH)_3$ nanoparticles adhered to the external surface of the clay after washing with water, they were completely desorbed by 2 M KOH. Taken together, these observations imply a different kind of interaction between the guest and host for $Rh(OH)_3/Ca_2Nb_3O_{10}$.

It has been reported that Rh_2O_3 and Nb_2O_5 react at 700–900 °C to give $RhNbO_4$, a rutile structure oxide containing Rh−O−Nb linkages.[17] We hypothesized that $Rh(OH)_3$ and Rh_2O_3 nanoparticles could be anchored to the $Ca_2Nb_3O_{10}$ by similar covalent bonds. Figure 4 shows XPS spectra in the Rh 3d region for $Rh(OH)_3/KCa_2Nb_3O_{10}$ (10

Scheme 1. Schematic Drawing of Exfoliation, Intercalation of $Rh(OH)_3$ Nanoparticles, and Flocculation

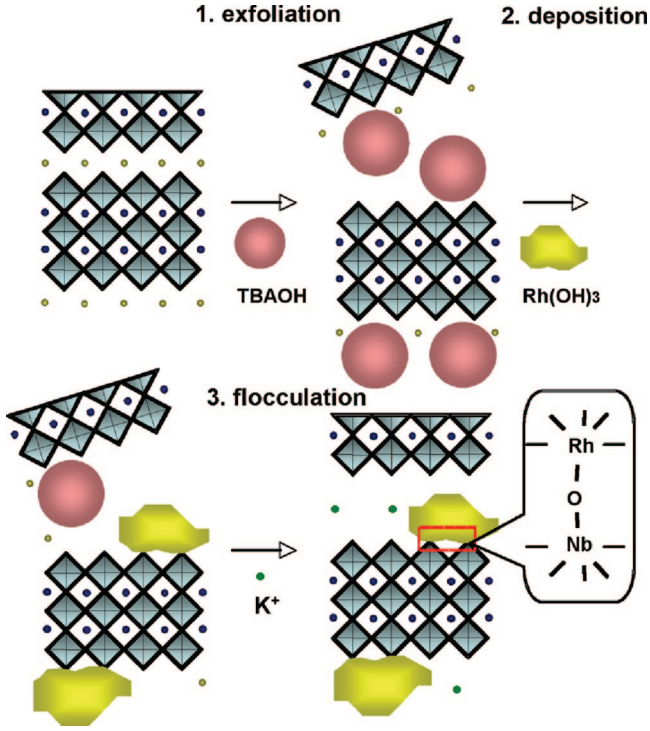

wt %), $Rh_2O_3/KCa_2Nb_3O_{10}$(10 wt %), and as-prepared $Rh(OH)_3$ particles. The Rh $3d_{5/2}$ peak for $Rh(OH)_3$ appears at 309.6 eV. After intercalation of $Rh(OH)_3$, the peak shifts slightly to 309.8 eV. The Rh $3d_{5/2}$ peak for Rh_2O_3 is typically observed at 308.1[17b] or 308.4 eV[5b] These binding energies are easily distinguished from that of Rh metal (306.5 eV[17b]). Although intercalated $Rh(OH)_3$ nanoparticles are transformed to Rh_2O_3 by calcination in air, the Rh $3d_{5/2}$ peak remains at high binding energy (309.4 eV). The Rh $3d_{5/2}$ peak for $RhNbO_4$ is at 309.1 eV,[17b] which is close to the binding energy observed in $Rh_2O_3/KCa_2Nb_3O_{10}$. Although they are not definitive, the XPS data are consistent with the picture of trivalent Rh anchored to the surface of the Nb-oxide layer through covalent Rh−O−Nb bonds, as sketched in Scheme 1.

Photocatalysis. The activity of $Rh(OH)_3$/ and $Rh_2O_3/KCa_2Nb_3O_{10}$ composites as photocatalysts for hydrogen evolution was measured using 10 vol % aqueous methanol solutions under 300 W Xe lamp irradiation. Figure 5 shows the time course of hydrogen evolution on flocculated $KCa_2Nb_3O_{10}$ (fl-$KCa_2Nb_3O_{10}$), $Rh(OH)_3/KCa_2Nb_3O_{10}$ at different Rh loadings (0.1, 1.0, 10.0 wt %), and $Rh_2O_3/KCa_2Nb_3O_{10}$ (0.1 wt %). With fl-$KCa_2Nb_3O_{10}$ alone, H_2 gas was evolved very slowly (51 μmol/h per 1 g of catalyst). The rate was approximately five times higher (275 μmol/h) using $Rh(OH)_3/KCa_2Nb_3O_{10}$ (0.1 wt %). Interestingly, the H_2 evolution rate decreased with increasing $Rh(OH)_3$ loading up to 10 wt %. This may be due in large part to an inner filter effect in which strongly UV-absorbing $Rh(OH)_3$ prevents light absorption by the semiconducting niobate sheets. However, on the basis of the extinction coefficient of aqueous $Rh(OH)_3$ at 350 nm ($\sim 1 \times 10^2$ M^{-1} cm^{-1}),[11] the loss in photocatalytic activity is not explained entirely by

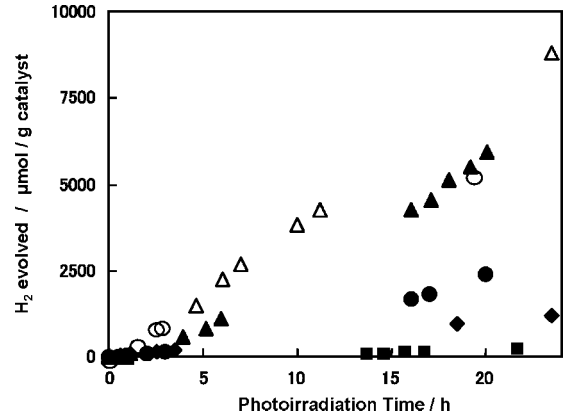

Figure 5. Time course of hydrogen generation from aqueous 10 wt % methanol solutions on fl-$KCa_2Nb_3O_{10}$ (solid diamonds), $Rh(OH)_3/KCa_2Nb_3O_{10}$ (0.1 wt %) (solid triangles), (1.0 wt %) (solid circles), (10 wt %) (solid squares), $Rh_2O_3/KCa_2Nb_3O_{10}$ (0.1 wt %) (open triangles), and $Pt/KCa_2Nb_3O_{10}$ (0.19 wt %) (open circles).

this effect. We estimate that at 10% loading (0.25 mg of Rh per mL of suspension, or about 2.4 mM $Rh(OH)_3$), about 40% of the UV light is absorbed by $Rh(OH)_3$. In contrast, the photocatalytic activity changes by a factor of 30 between 0.1% and 10% loading of $Rh(OH)_3$ nanoparticles.

Comparing different nanoparticle catalysts ($Rh(OH)_3$, Rh_2O_3, and Pt), we find that $Rh_2O_3/KCa_2Nb_3O_{10}$ (0.1 wt %) is a better catalyst than $Rh(OH)_3/KCa_2Nb_3O_{10}$ at the same loading. Pt nanoparticles were also dispersed onto the surface of the niobate sheets by photoreduction in aqueous H_2PtCl_6 solution,[18] and the Pt loaded sheets were collected by flocculation with KOH solution. The hydrogen evolution rate for composites loaded with 0.19 wt % Pt (which are considered to be very active photocatalysts) was only about 70% of that of $Rh_2O_3/KCa_2Nb_3O_{10}$ (0.10 wt %), which contains an equimolar amount of catalytic metal. Another difference between the properties of the Pt- and Rh-loaded catalysts is a 1–2 h induction period for hydrogen evolution in the latter case. This is most evident for the less active catalysts, e.g., $Rh(OH)_3/KCa_2Nb_3O_{10}$, as seen in Figure 5. The induction period likely represents the reduction of Rh(III) to Rh(0), as evidenced by a gradual color change of the 10 wt % sample (solid squares in Figure 5) from yellow to gray.

Domen et al. have shown that proton exchanged $HCa_2Nb_3O_{10}$ and $H_{4-x}K_xNb_6O_{17}$ have much higher activity as photocatalysts for hydrogen evolution from methanol solutions than $HCa_2Nb_3O_{10}$ and $K_4Nb_6O_{17}$ because the reactants (water and methanol) have better access to the more hydrated interlayer galleries[19] Proton exchanged $Rh_2O_3/KCa_2Nb_3O_{10}$ was obtained by washing twice with 1 N aqueous HNO_3 solution. The acid treated catalysts are abbreviated $Rh_2O_3/HCa_2Nb_3O_{10}(n)$ and fl-$HCa_2Nb_3O_{10}$. XRD patterns of $Rh_2O_3/HCa_2Nb_3O_{10}$ (1.0 wt %) and fl-$HCa_2Nb_3O_{10}$ show that the basal spacings expand 0.15 nm after acid treatment, consistent with increased hydration of the interlayer galleries. Figure 6 shows photocatalytic activity before and after acid exchange. The rate of hydrogen evolution from fl-$HCa_2Nb_3O_{10}$ is almost seven times higher than from fl-$KCa_2Nb_3O_{10}$. $Rh_2O_3/HCa_2Nb_3O_{10}$ (1.0 wt %) is a substantially better photocatalyst than $Rh_2O_3/KCa_2Nb_3O_{10}$ (1.0 wt

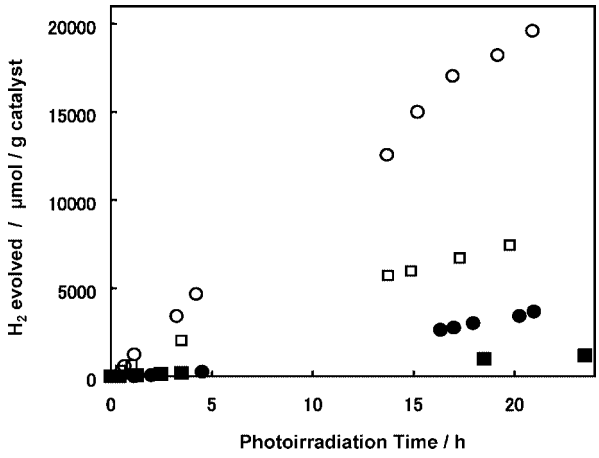

Figure 6. Time course of hydrogen evolution from aqueous 10 wt % methanol solutions at fl-$KCa_2Nb_3O_{10}$ and $Rh_2O_3/KCa_2Nb_3O_{10}$ (1.0 wt %) before and after proton exchange: fl-$KCa_2Nb_3O_{10}$ (solid squares), fl-$HCa_2Nb_3O_{10}$ (open squares), $Rh_2O_3/KCa_2Nb_3O_{10}$ (1.0 wt %) (solid circles), and $Rh_2O_3/HCa_2Nb_3O_{10}$ (1.0 wt %) (open circles).

%), with a 6-fold increase in hydrogen evolution rate. It is also important to note that $Rh_2O_3/HCa_2Nb_3O_{10}$ is stable below pH 4.0, whereas the less active catalyst $Rh(OH)_3/HCa_2Nb_3O_{10}$ is not. Thus, $Rh_2O_3/HCa_2Nb_3O_{10}$ may be a useful component of overall water splitting systems that operate at acidic pH.

In conclusion, well-dispersed $Rh(OH)_3$ nanoparticles were intercalated into the interlayer galleries of a Dion−Jacobson type layered perovskite ($KCa_2Nb_3O_{10}$). Calcination transformed intercalated $Rh(OH)_3$ to well dispersed Rh_2O_3 nanoparticles. Zeta potential, ion-exchange, and XPS experiments point to covalent Rh−O−Nb bonding as the mode of anchoring the nanoparticles to the sheets. The evidence for this bonding is indirect, and further structural studies by NMR and X-ray absorption are currently contemplated. $Rh_2O_3/HCa_2Nb_3O_{10}$ was found to be a very active photocatalyst in aqueous 10% methanol, consistent with the small size the nanoparticles and their uniform dispersion on the niobate sheets. These covalently bound catalytic clusters are insensitive to cation exchange under acidic or basic conditions, suggesting that they may be useful in overall water splitting schemes.

Recently, Domen and co-workers have found that Rh−Cr mixed oxide ($Rh_{2-y}Cr_yO_3$) nanoparticles supported on $(Ga_{1-x}Zn_x)(N_{1-x}O_x)$ catalyze overall water splitting under visible light. The $Rh_{2-y}Cr_yO_3$ clusters catalyze hydrogen evolution and are remarkably insensitive to the presence of oxygen.[5] Preliminary experiments show that $Rh(OH)_3$/ and $Rh_2O_3/KCa_2Nb_3O_{10}$ are not active for overall water splitting with UV irradiation and that they catalyze the recombination of H_2 and O_2 into water. It is possible that by covering the supported Rh_2O_3 nanoparticles with Cr_2O_3 in a core–shell arrangement, $Rh_2O_3/KCa_2Nb_3O_{10}$ or $Rh_2O_3/HCa_2Nb_3O_{10}$ might be converted to a water splitting catalyst by inhibiting the recombination reaction. Synthetic experiments along these lines are currently in progress.

Acknowledgment. This research was supported by the Department of Energy under grant DE-FG02-07ER15911. We thank Henry Gong for carrying out the ICP-AES analysis. H.H. thanks Shiseido Co. Ltd. for giving him the opportunity to study at the Pennsylvania State University and for financial support. W.J.Y. thanks the donors of the ACS Petroleum Research Fund for support in the form of a postdoctoral fellowship.

Supporting Information Available: Experimental details, analytical results, XRD patterns of $Rh(OH)_3$, $Rh(OH)_3/KCa_2Nb_3O_{10}$ at saturation loading, and $Rh(OH)_3/KCa_2Nb_3O_{10}$ without photoirradiation, FT-IR spectra of TBAOH/$KCa_2Nb_3O_{10}$, $Rh(OH)_3/Ca_2Nb_3O_{10}$ at saturated loading washed with water, and $Rh(OH)_3/KCa_2Nb_3O_{10}$ (10 wt %), pH dependence of the ζ potential of $Rh(OH)_3$ particles, and XRD patterns of $Rh(OH)_3$/F-mica before and after intercalation. This material is available free of charge via the Internet at http://pubs.acs.org.

References

(1) Fujishima, A.; Honda, K. *Nature* **1972**, *238*, 37.
(2) Bard, A. J.; Fox, M. *Acc. Chem. Res.* **1995**, *28*, 141.
(3) (a) For example, Domen, K.; Naito, S.; Soma, M.; Ohishi, T.; Tamaru, K. *J. Chem. Soc., Chem. Commun.* **1980**, 543. (b) Domen, K.; Kudo, A.; Shinozaki, A.; Tanaka, A.; Maruya, K.; Onishi, T. *J. Chem. Soc., Chem. Commun.* **1986**, 356. (c) Kudo, A.; Tanaka, A.; Domen, K.; Maruya, K.; Aika, K.; Onishi, T. *J. Catal.* **1988**, *111*, 67.
(4) (a) Inoue, Y.; Kubokawa, T.; Sato, K. *J. Chem. Soc., Chem. Commun.* **1990**, 1298; *J. Phys. Chem.* **1991**, *95*, 4059. (b) Maeda, K.; Takata, T.; Hara, M.; Saito, N.; Inoue, Y.; Kobayashi, H.; Domen, K. *J. Am. Chem. Soc.* **2005**, *127*, 8286.
(5) (a) Maeda, K.; Teramura, K.; Lu, D.; Takata, T.; Saito, N.; Inoue, Y.; Domen, K. *Nature* **2006**, *404*, 295; *J. Phys. Chem. B* **2006**, *110*, 13753. (b) Maeda, K.; Teramura, K.; Masuda, H.; Takata, T.; Saito, N.; Inoue, Y.; Domen, K. *J. Phys. Chem. B* **2006**, *110*, 13107.
(6) (a) Maeda, K.; Teramura, K.; Lu, D.; Saito, N.; Inoue, Y.; Domen, K. *Angew. Chem., Int. Ed* **2006,** *45,* 7806; *J. Phys. Chem. C* **2007**, *111*, 7554.
(7) (a) For example, Sayama, K.; Tanaka, A.; Domen, K.; Maruya, K.; Onishi, T. *J. Phys. Chem.* **1991**, *95*, 1345. (b) Kim, Y. I.; Salim, S.; Huq, M. J.; Mallouk, T. E. *J. Am. Chem. Soc.* **1991**, *113*, 9561.
(8) (a) For example, Kim, Y. I.; Atherton, S. J.; Brigham, E. S.; Mallouk, T. E. *J. Phys. Chem.* **1993**, *97*, 11802. (b) Domen, K.; Yoshimura, J.; Sekine, T.; Tanaka, A.; Onishi, T. *Catal. Lett.* **1990**, *4*, 339. (c) Takata, T.; Furumi, Y.; Shinohara, K.; Tanaka, A.; Hara, M.; Kondo, J. N.; Domen, K. *Chem. Mater.* **1997**, *9*, 1063.
(9) (a) Ebina, Y.; Sasaki, T.; Harada, M.; Watanabe, M. *Chem. Mater.* **2002**, *14*, 4390. (b) Ebina, Y.; Sakai, N.; Sasaki, T. *J. Phys. Chem. B* **2005**, *109*, 17212.
(10) Hata, H.; Kubo, S.; Kobayashi, Y.; Mallouk, T. E. *J. Am. Chem. Soc.* **2007**, *129*, 3064.
(11) (a) Armstrong, J. C.; Choppin, G. R. *Radiochemistry of Rhodium*; United States Atomic Energy Commission, 1965; (b) Jorgensen, C. K. *Acta Chem. Scand.* **1956**, *10*, 500.
(12) Ebina, Y.; Tanaka, A.; Kondo, J. N.; Domen, K. *Chem. Mater.* **1996**, *8*, 2534.
(13) Fang, M.; Kim, C. H.; Mallouk, T. E. *Chem. Mater.* **1999**, *11*, 1519.
(14) Kim, T. W.; Hur, S. G.; Hwang, S.-J.; Park, H.; Choi, W.; Choy, J.-H. *Adv. Funct. Mater.* **2007**, *17*, 307.
(15) $Rh(OH)_3$ nanoparticles were synthesized as followed. To 6.32 mL of $RhCl_3$ aqueous solution (20 mM) was added 50 mL of 25 mM of TBAOH aqueous solution, and the mixture was stirred for 1 h. The precipitated yellow powder was collected by centrifugation and washed with water. Finally, the sample was dried at 333 K.
(16) Sodium fluortetrasilicic mica with the chemical formula $Na_{0.66}Mg_{2.68}(Si_{3.98}Al_{0.02})O_{10.02}F_{1.96}$ and a cation exchange capacity (CEC) of 120 mequiv/100 g (ME-100, CO-OP Chemicals) was used.

(17) (a) Hu, Z.; Nakamura, H.; Kunimori, K.; Asano, H.; Uchijima, T. *J. Catal.* **1988**, *112*, 478. (b) Kunimori, K.; Hu, Z.; Uchijima, T.; Asakura, K.; Iwasawa, Y.; Soma, M. *Catal. Today* **1990**, *8*, 85.
(18) (a) Kraeutler, B.; Bard, A. J. *J. Am. Chem. Soc.* **1978**, *100*, 4317. (b) Compton, O. C.; Carroll, E. C.; Kim, J. Y.; Larsen, D. S., Osterloh, F. E. *J. Phys. Chem. C* **2007**, *111*, 14589..
(19) (a) Domen, K.; Kudo, A.; Shibata, M.; Tanaka, A.; Maruya, K.; Onishi, T. *J. Chem. Soc., Chem. Commun.* **1986**, 1706. (b) Domen, K.; Ebina, Y.; Sekine, A.; Tanaka, A.; Kondo, J.; Hirose, C. *Catal. Today* **1993**, *16*, 479.

NL072571W